AI-Assisted Characterization of Coronary High-Risk Plaques in Troponin-Negative Patients Presenting with Atypical Chest Pain: A 256-Slice CCTA Analysis

Thunnawat Wattanaseth, MD, MSc, PhD[1], Phawit Norchai, MD, MSc, PhD[1], Mart Maiprasert, MD, PhD[1], Peerapong Prabhakornritta, MD, MSc[1], Patana Teng-umnuay, MD, PhD[1], Pansak Sugkraroek, MD[1]

[1] Department of Anti-Aging and Regenerative Medicine, College of Integrative Medicine (CIM), Dhurakij Pundit University, Bangkok, Thailand

Abstract

Background: While coronary computed tomography angiography (CCTA) is an established modality for evaluating chest pain, there is limited up-to-date data on the utility of advanced artificial intelligence (AI)-assisted cardiac software utilizing 256-slice computed tomography (CT) scans to systematically detect and characterize specific high-risk plaque features (HRPF) in the clinical subset of patients with atypical chest pain and troponin-negative (TNEG).

Objective: To analyze the characteristics of coronary artery HRPF on CCTA using AI-assisted software and a 256-slice CT scanner in patients presenting with atypical chest pain and TNEG.

Materials and Methods: A retrospective analysis was conducted on 118 eligible TNEG patients with documented coronary plaques who underwent CCTA between January 2020 and April 2024. Data were retrieved via the Picture Archiving and Communication System (PACS) and Hospital Information System (HIS). Coronary artery plaque analysis was performed using AI-assisted cardiac software (Cardiac Suite) on a 256-slice CT scanner. The presence and types of HRPF were evaluated, including: 1) low-attenuation plaque (<30 Hounsfield units), 2) positive remodeling, 3) spotty calcification, and 4) the napkin-ring sign. Statistical analyses were performed using the unpaired t-test, chi-square test, and Cramer's V to determine associations between variables.

Results: Of the 118 cases evaluated, obstructive coronary artery disease (CAD) was identified in 66 cases (56.0%) and non-obstructive CAD in 52 cases (44.0%). HRPF were significantly more prevalent in the obstructive CAD group (43/66 cases, 65.2%) compared to the non-obstructive CAD group (5/52 cases, 9.6%). The AI-assisted software efficiently identified and characterized plaque morphology. Low-attenuation plaque was the most common HRPF characteristic, observed in 38 cases (32.2%), predominantly within obstructive lesions (stenosis >50%). A high coronary artery calcium score (CACS >300, percentiles P3 and P4) demonstrated a strong, statistically significant association with HRPF, present in 51 cases (43.2%). Based on these data, it is hypothesized that the transition from P2 (CACS 101-300) to P3/P4 (CACS >300) corresponds to a biological shift from non-HRPF to HRPF. Notably, a 36-year-old male smoker presented with distinct obstructive HRPF despite a CACS of 0.

Conclusion: AI-assisted cardiac software provides rapid, precise identification and characterization of coronary plaques, particularly vulnerable HRPF. Upgrading CT infrastructure with integrated AI-assisted analysis tools significantly enhances diagnostic accuracy. This software acts as a crucial clinical decision-making aid to accurately rule out or confirm coronary etiologies in patients presenting with atypical chest pain and TNEG.

Keywords: AI-assisted cardiac software; Cardiac suite; High-risk plaque features (HRPF); Atypical chest pain; Troponin-negative

Received 5 February 2026 | Revised 27 June 2026 | Accepted 15 July 2026

J Med Assoc Thai 2026;109(8):681-8

https://doi.org/10.35755/jmedassocthai.2026.8.04008

Over the past five years, advanced artificial intelligence (AI)-assisted cardiac software has undergone rapid development, fundamentally transforming cardiovascular imaging. Despite these technological leaps, many computed tomography (CT) centers operating older-generation scanners continue to utilize outdated post-processing software. These legacy

Correspondence to:

Wattanaseth T.
Department of Anti-Aging and Regenerative Medicine, College of Integrative Medicine (CIM), Dhurakij Pundit University, Bangkok 10210, Thailand.
Phone: +66-95-8796999
Email: Thunnawat.wat@dpu.ac.th
ORCID: 0000-0002-1787-5781

How to cite this article:

Wattanaseth T, Norchai P, Maiprasert M, Prabhakornritta P, Teng-umnuay P, Sugkraroek P. AI-Assisted Characterization of Coronary High-Risk Plaques in Troponin-Negative Patients Presenting with Atypical Chest Pain: A 256-Slice CCTA Analysis. J Med Assoc Thai 2026;109:681-8.

What is already known about this topic?

CCTA combined with AI-assisted software provides an effective method for analyzing the morphologic types of HRPF within coronary arteries, especially obstructive HRPF.

What does this study add?

Based on this report, it is hypothesized that the transition from P2 (CACS 101-300) to P3/P4 (CACS >300) corresponds to a biological shift from non-HRPF to HRPF.

systems lack integrated AI capabilities that allow for the precise identification, automated quantification, and geometric characterization of coronary artery disease (CAD). This technological gap is particularly problematic when evaluating patients presenting with atypical chest pain, where establishing a definitive diagnosis remains clinically challenging.

In the emergency department (ED), chest pain is one of the most frequent complaints[1]. While a definitive etiology may not be immediately identifiable, emergency clinicians must rapidly rule out life-threatening conditions. The top five critical cardiovascular and thoracic causes of chest pain that require immediate triage[1] include:

1. Acute coronary syndrome (ACS)/myocardial infarction (MI)
2. Aortic dissection
3. Pulmonary embolism
4. Tension pneumothorax
5. Cardiac tamponade

Atypical chest pain is characterized by symptoms that meet only one or two of these criteria, often presenting as pleuritic, sharp, burning, or epigastric discomfort, or manifesting solely as dyspnea, diaphoresis, or unexplained fatigue. Literature indicates that ACS presents with typical chest pain in approximately 80% of cases, whereas an estimated 20% of patients manifest with atypical symptoms. Because atypical presentations are highly prevalent—especially among women, elderly individuals, and diabetic patients—it is imperative that life-threatening coronary pathologies are not missed during initial triage.

This diagnostic challenge is highly pronounced in patients presenting with atypical chest pain who demonstrate troponin-negative (TNEG) biomarkers. TNEG status often temporarily misleads clinicians into ruling out acute myocardial necrosis; however, underlying unstable coronary atheroma may still be present. Indeed, coronary artery stenosis leading to silent or atypical myocardial ischemia remains one of the top five causes of chest pain in individuals aged 45-64 years[2-5]. In this specific patient cohort, coronary computed tomography angiography (CCTA) provides exceptional negative predictive value to safely exclude obstructive CAD.

Crucially, standard luminal evaluation alone may overlook non-obstructive yet highly vulnerable plaques. High-risk plaques, or unstable plaques, possess a high propensity for rupture, erosion, and subsequent acute luminal thrombosis, leading to catastrophic ACS or sudden cardiac death. Histologically, these vulnerable features typically consist of small, spotty calcifications and a large lipid-rich necrotic core covered by a thin, vulnerable fibrous cap, structurally classified as a thin-cap fibroatheroma (TCFA)[6,7]. On CCTA, advanced software allows for the qualitative and quantitative identification of four distinct morphologic high-risk plaque features (HRPF):

1. Low-attenuation plaque: Characterized by a large lipid- or necrotic-rich core demonstrating a CT attenuation value of <30 Hounsfield units (HU). The presence of low-attenuation plaque has been strongly correlated with plaque instability and a significantly higher incidence of ACS[8-11].

2. Positive remodeling: Defined as a compensatory outward enlargement of the vessel wall at the atherosclerotic site. This mechanism preserves the internal luminal area despite a high plaque burden. Histologically, positively remodeled plaques exhibit higher lipid content and an abundance of inflammatory macrophages[8-11].

3. Spotty calcification: Defined as small, focal calcified elements measuring <3 mm in size. On CCTA, these microcalcifications are widely recognized markers of active plaque inflammation and instability compared to large, stable macrocalcifications[8-11].

4. The napkin-ring sign: A highly specific, qualitative CCTA feature characterized by a central low-attenuation necrotic core immediately adjacent to the patent coronary lumen, bounded by a higher-attenuation peripheral ring-like tissue zone representing the fibrous plaque capsule[8-11].

Given the clinical necessity of identifying these hidden features before a major ischemic event occurs, there is an urgent need to evaluate how modern image processing impacts clinical workflows. Therefore, the aim of this study was to analyze the characteristics of coronary artery HRPF using advanced, AI-assisted CCTA software on a 256-slice CT scanner in patients presenting with atypical chest pain and TNEG biomarkers.

Objective

The aim of this study was to evaluate the phenotypic characteristics and anatomical distribution of coronary artery HRPF using advanced AI-assisted CCTA software in patients presenting with atypical chest pain and TNEG biomarkers.

Materials and Methods

Study Design and Population

This study was a retrospective, single-center analysis of patients presenting with atypical chest pain

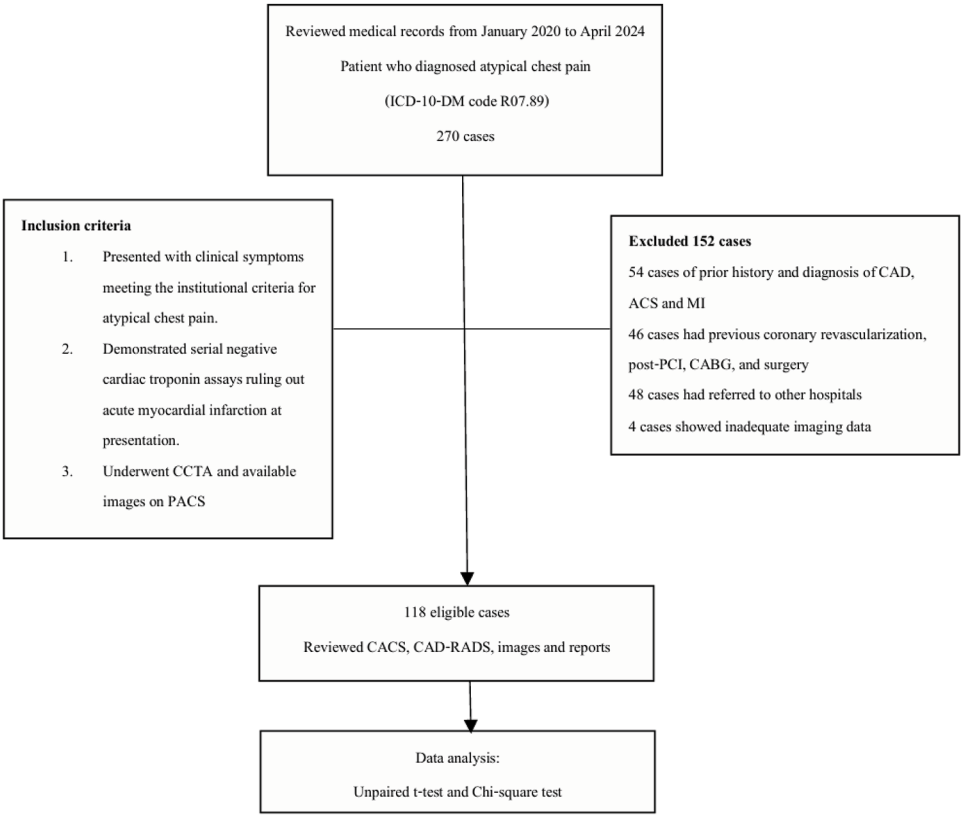

Figure 1. Flow study chart.

(ICD-10-DM code R07.89) and TNEG biomarkers. The study cohort comprised 118 eligible cases identified through a comprehensive electronic medical record search spanning from January 2020 to April 2024. Relevant clinical, biochemical, and radiological data documents were systematically retrieved via the Institutional Hospital Information System (HIS) and the Picture Archiving and Communication System (PACS), as seen in Figure 1.

Inclusion criteria consisted of patients who:

1. Presented with clinical symptoms meeting the institutional criteria for atypical chest pain.

2. Demonstrated serial negative cardiac troponin assays ruling out acute MI at presentation.

3. Underwent a comprehensive CCTA examination, and the available images on PACS

Exclusion criteria: Patients meeting any of the following criteria were excluded from the study:

1. Prior history of CAD: Known cases of established CAD, including patients with a history of documented ACS or MI prior to the index presentation.

2. Previous coronary revascularization: Status post-percutaneous coronary intervention (PCI) with coronary stent placement, or status post-coronary artery bypass graft (CABG) surgery.

3. Inadequate Imaging Data: Technical failure during CCTA acquisition, severe motion or breathing artifacts rendering the scan uninterpretable, or otherwise unavailable imaging datasets within the PACS.

Computed Tomography Acquisition Protocol

All eligible participants underwent CCTA examinations performed on a 256-slice multidetector CT scanner (Brilliance iCT, Philips Healthcare) with advanced AI-assisted cardiac software (Cardiac Suit) utilizing a standardized institutional CCTA acquisition protocol.

Prospective or retrospective electrocardiogram (ECG) gating was applied based on the patient's resting heart rate to optimize temporal resolution and minimize radiation dose. In patients with an initial heart rate greater than 65 beats per minute, oral beta-blockers were administered prior to the scan.

A non-ionic, high-concentration iodinated contrast medium was injected intravenously via an automated power injector through an antecubital vein, bolus flow rate 5ml/sec, followed by a saline flush. Bolus tracking

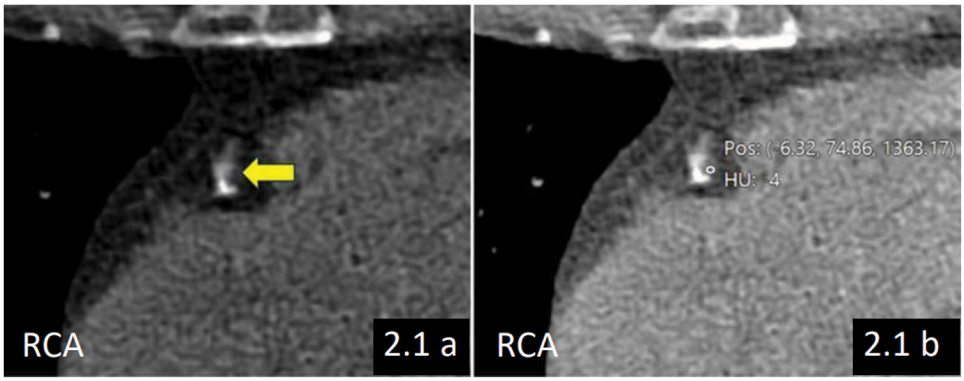

Figure 2. Low attenuation plaque. (2.1a, b) Cross-sectional luminal analysis of the right coronary artery (RCA) showed a focal intraluminal low attenuation plaque (yellow arrow) in the middle segment of the RCA, representing the lipid-rich core. The quantitative measurement of the plaque density=4 HU.

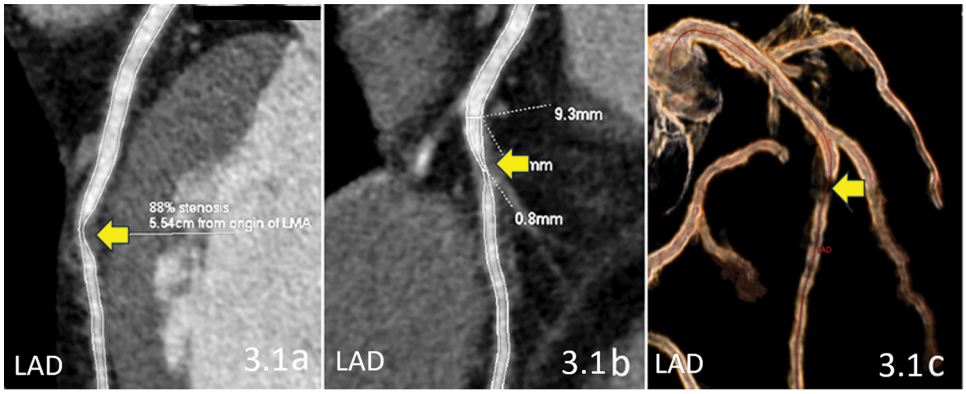

Figure 3. Positive remodeling plaque with an intraluminal low-attenuation plaque. (3.1a, b) Multi-planar reconstruction and analysis of the left anterior descending coronary artery (LAD) showed a focal outward enlargement of the low-density plaque (yellow arrow) at the middle segment LAD, representing the positive remodeling. (3.1c) 3D VRT vessel wall and luminal analysis showed a co-existing "filling defect" of an intraluminal low-attenuation plaque, causing a narrow LAD lumen.

was used to initiate scan acquisition, with the region of interest (ROI) placed in the lumen of the ascending aorta. All images were acquired during a single breath-hold at mid-inspiration.

CCTA Image Post-Processing and Plaque Characterization

The acquired CCTA datasets were transferred to a dedicated workstation and analyzed using advanced, AI-assisted cardiac post-processing software (Cardiac Suite, Philips Healthcare). The software executed automated multiplanar reconstructions (MPR), curved planar reformations (CPR), and cross-sectional vessel centerline extractions across all major coronary artery segments in accordance with the Society of Cardiovascular Computed Tomography (SCCT) guidelines.

The advanced cardiac software provided automated segmentation, volumetric quantification, and morphologic profiling of coronary atherosclerotic plaques. Coronary plaques were systematically evaluated and classified based on the presence of four established HRPF, seen in Figure 2-5.

To ensure diagnostic accuracy and eliminate potential software segmentation artifacts, board-certified radiologists reviewed and verified all AI-generated outputs. The final expert consensus approved all automatic lumen boundaries, calculated degrees of luminal stenosis, anatomical segment localizations, and the definitive qualitative presence or absence of HRPF markers.

CAD-RADS

CAD-RADS was used for determining the coronary features. CAD-RADS stands for Coronary Artery Disease Reporting and Data System[12], which

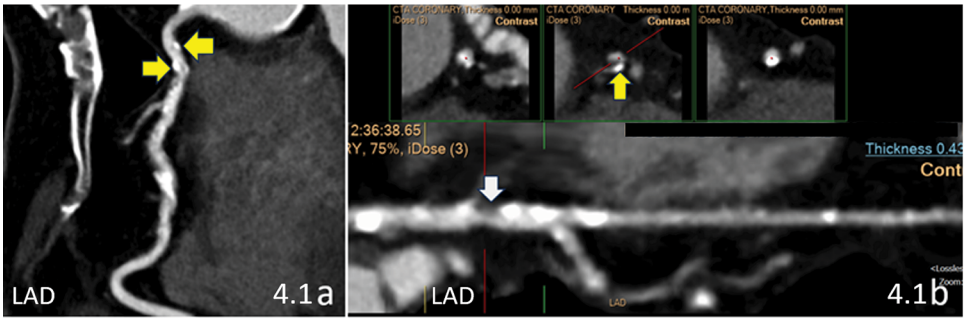

Figure 4. Spotty calcification. (4.1a, b) Multi-planar reconstruction and analysis of the left anterior descending coronary artery (LAD) showed a few spotty calcifications (yellow arrows) at the proximal LAD. A spotty calcification associated with low-attenuation plaque (white arrow), causing luminal stenosis.

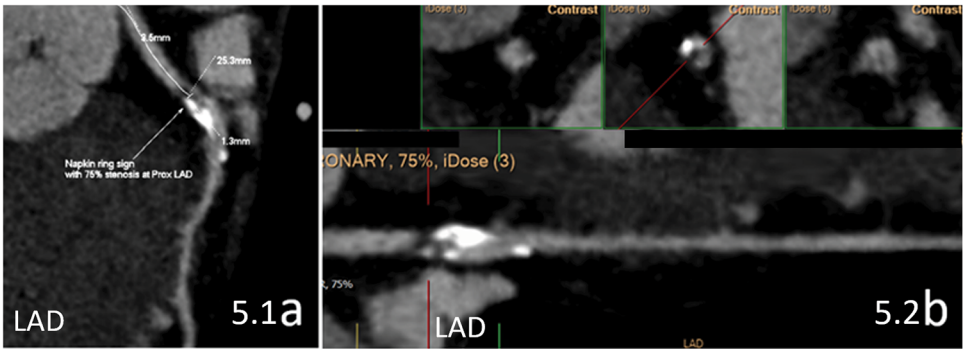

Figure 5. The napkin-ring sign. (5.1a, b) Multi-planar reconstruction and analysis showed a focal black density "filling-defect" in the proximal LAD, representing a central low-density area (necrotic core) with a higher "ring-like" plaque surrounding the central necrotic core.

was used for analyzing features on the coronary artery, as follows:

1. The degrees of coronary artery stenosis (0% stenosis: CAD-RADS 0, 1% to 24% stenosis: CAD-RADS 1, 25% to 49% stenosis: CAD-RADS 2, 50% to 69% stenosis: CAD-RADS 3, 70% to 99% stenosis: CAD-RADS 4, and 100% stenosis: CAD-RADS 5)

2. The degrees of coronary artery calcium score (CACS) (1-100: P1, 101-300: P2, 301-999: P3, and >1,000: P4)

3. The patterns of HRPF consist of the low attenuation plaque (<30 HU), positive remodeling, spotty calcification (density >130 HU and a diameter of <3.0 mm), and napkin-ring sign

Cardiovascular Risk Stratification

The Framingham Risk Score (FRS) was utilized in this study to estimate the 10-year risk of developing cardiovascular disease (CVD). The FRS was specifically selected over the regional Thai Cardiovascular (Thai CV) Risk Score because the FRS algorithm incorporates the clinical use of antihypertensive medication as an active variable. Given that antihypertensive therapies are established to modulate and slow the progression of coronary atherosclerosis. A parameter not explicitly factored into the standard Thai CV risk model.

The parameters required to calculate the 10-year FRS for cardiovascular disease consist of age, sex, total cholesterol, high-density lipoprotein (HDL), systolic blood pressure, antihypertensive drug (yes/no), current smoking status (yes/no), and diabetes mellitus status (yes/no).

FRS has three distinct risk categories: 1) Low cardiovascular risk: FRS <10%, 2) Intermediate cardiovascular risk: 10% ≤ FRS ≤ 19%, and 3) High cardiovascular risk: FRS ≥20%.

Statistical Analysis

Statistical analyses were performed using standard medical statistical software. Descriptive statistics were utilized to summarize the baseline clinical and imaging data. The non-normally distributed continuous variables were presented as median with interquartile

ranges (IQR). Categorical variables, including the prevalence of underlying disease, specific HRPF and FRS categories, were expressed as absolute frequencies and percentages.

To evaluate differences between groups:

1. An unpaired t-test was used to compare continuous variables between independent groups (obstructive vs. non-obstructive CAD).

2. Chi-square test of independence was applied to determine the statistical significance of associations between categorical variables (e.g., the relationship between CACS and the presence of HRPF).

3. Cramer's V was calculated following significant chi-square tests to quantify the strength of the association between the categorical variables, interpreted on a scale from 0 (no association) to 1 (perfect association).

For all statistical evaluations, a two-tailed p-value of less than 0.05 was considered to indicate a statistically significant difference.

Ethical Consideration

The research was approved by the Human Research Ethics Review Board of Dhurakij Pundit University (Code: DPUHREC003/67FB COA015/67).

Results

The study cohort comprised 118 eligible cases with a median age of 58 years (range 24-90) and a median BMI of 26.18 kg/m² (IQR 22.8-28.8). The sample was 49.2% male (58 cases).

The prevalence of comorbidities was as follows: hypertension (61.0%, 72 cases), dyslipidemia (22.0%, 26 cases), diabetes mellitus (15.2%, 18 cases), and smoking (8.4%, 10 cases). FRS were distributed as follows: low (27.1%, 32 cases), intermediate (62.7%, 74 cases), and high (10.1%, 12 cases). Baseline characteristics are summarized in Table 1.

Of the 118 cases evaluated, obstructive CAD was identified in 66 cases (56.0%) and non-obstructive CAD in 52 cases (44.0%).

Table 1. Baseline characteristics of the eligible cases (n=118)

	Value
Age (years); median [range]	58 [24-90]
Male; n (%)	58 (49.2)
Body mass index (kg/m^2); median [IQR]	26.18 [22.8-28.8]
Diabetes; n (%)	18 (15.2)
Hypertension; n (%)	72 (61.0)
Dyslipidemia; n (%)	26 (22.0)
Smoking; n (%)	10 (8.4)
Framingham Risk Score; n (%)	
Low (<10%)	32 (27.1)
Intermediate (<10% to 19%)	74 (62.7)
High (≥20%)	12 (10.1)

IQR=interquartile range

HRPF were identified in 48 cases (40.7% of the total cohort), of which 43 (89.5%) were associated with obstructive CAD (stenosis >50%). The specific types of HRPF observed were low-attenuation plaque (32.2%, 38 cases), spotty calcification (5.1%, 6 cases), positive remodeling (1.7%, 2 cases), and the napkin-ring sign (1.7%, 2 cases) (Table 2).

Representative images of these four HRPF types are presented in Figure 2-5. Obstructive HRPF was significantly associated with low-attenuation plaque (Table 2, 3). The distribution of obstructive CAD (stenosis >50%) by segment was as follows: proximal left anterior descending (LAD) artery (28.8%, 34 cases), proximal right coronary artery (RCA) (22.7%, 15 cases), mid-LAD (6.8%, 8 cases), and left main coronary artery (LMCA) (4.2%, 5 cases) (Table 3).

Finally, a strong association was observed between the presence of HRPF and elevated CACS (>300, P3 and P4) (Table 4).

Discussion

Low-attenuation plaque represents the most prevalent characteristic of HRPF and can be effectively identified using advanced AI-assisted CCTA software. The study identified 45 cases (38%) of atypical chest

Table 2. Association between the types of high-risk plaque feature (HRPF) and the affected coronary artery (n=48)

Coronary artery	Low attenuation plaque	Positive remodeling	Spotty calcification	Napkin-ring sign	p-value
Right coronary artery; n (%)	10 (20.8), Obstructive CAD	0 (0.0)	1 (2.0)	0 (0.0)	<0.001*
Left main coronary artery; n (%)	2 (4.1)	0 (0.0)	0 (0.0)	0 (0.0)	<0.001*
left anterior descending artery; n (%)	25 (58.3), Obstructive CAD	2 (4.1)	5 (10.4), Obstructive CAD	2 (4.1), Obstructive CAD	<0.001*
left circumflex artery; n (%)	1 (2.0), Obstructive CAD	0 (0.0)	0 (0.0)	0 (0.0)	<0.001*

CAD=coronary artery disease

χ^2=40.030, degree of freedom=9, Cramer's V=0.52

* p<0.05, statistical significance

Table 3. The rate of the obstructive CAD (stenosis ≥50%) in each affected coronary artery segment (n=118)

Affected coronary segment name(s)	Rate of obstructive CAD relative to all segments of stenosis (n=66, 55.9%)
Proximal right coronary artery; n (%)	15 (22.7)
Mid right coronary artery; n (%)	2 (1.7)
Left main coronary artery; n (%)	5 (4.2)
Proximal left anterior descending artery; n (%)	34 (28.8)
Mid left anterior descending artery; n (%)	8 (6.8)
Proximal left circumflex artery; n (%)	1 (1.7)

CAD=coronary artery disease

Table 4. Association between the high-risk plaque features (HRPF) and the coronary artery calcium score (CACS) (n=118)

HRPF	CACS					p-value
	0 (n=18)	1-100 [P1] Mild (n=13)	101-300 [P2] Moderate (n=36)	301-999 [P3] Severe (n=31)	≥1,000 [P4] Extensive (n=20)	
Presence of HRPF	1	1	2	25	20	<0.001*
Presence of non-HRPF	17	12	34	6	0	<0.001*

χ^2=288.913, degree of freedom=8, Cramer's V=0.75
* p<0.05, statistical significance

pain and TNEG status with high CACS (>300, P3 and P4), which were associated with HRPF.

Notably, 95.5% of cases exhibiting HRPF showed obstructive coronary artery stenosis (>50%). In contrast, the majority of cases (63, 53.4%) presented with non-HRPF and CACS between 0 and 300, peaking in the P2 range (CACS 101-300).

Based on these data, it is hypothesized that the transition from P2 (CACS 101-300) to P3/P4 (CACS >300) corresponds to a biological shift from non-HRPF to HRPF[12-15].

This aligns with recent findings by Mézquita et al. (2023), who demonstrated that CACS >300 is significantly associated with both obstructive CAD and HRPF[16]. Further research is required to establish a consensus on the critical CACS cut-off points marking this biological transition.

Our results demonstrate that AI-assisted software effectively identifies and characterizes HRPF on CCTA. In patients with atypical chest pain and TNEG—where distinguishing between acute MI and other etiologies is clinically challenging—CCTA serves as the gold standard for diagnosis and exclusion.

Consequently, AI-enhanced imaging is a crucial tool for accurate clinical decision-making in this patient population.

Conclusion

The HRPF of the coronary artery, typically low-attenuation plaque at proximal LAD, were significantly found in the case of atypical chest pain with TNEG, at the age of >50-year-old with intermediate to high cardiovascular risk. The high level of CACS >300 (P3 and P4) had strong significant association with an obstructive CAD (≥50% stenosis) and presence of HRPF. The follow up CCTA is the state-of-art, individually.

Acknowledgement

The authors gratefully acknowledge Kasemrad International Rattanathibeth Hospital for providing the facilities and support for data collection.

Authors contributions

TW is the corresponding author, head of project, main conceptual idea, data collection, calculation, analysis, and wrote the manuscript. PN, MM, PS, PT, and PP helped shape the manuscript and discussion of the results.

Clinical Trial Registration

Not applicable. This study is the non-clinical trial study.

Conflicts of interest

The authors declare no conflict of interest.

Data Availability Statement

The available data from HIS and PACS of Kassemrad International Rattanathibeth Hospital.

Ethics Approval and Consent to Participate

The research was approved by the Human Research Ethics Review Board of Dhurakij Pundit University (Code: DPUHREC003/67FB COA015/67).

Funding Disclosure

The authors received no financial support for the research, authorship, and/or publication of this article.

Use of Artificial Intelligence

This article used AI (Gemini) for grammar improvement.

References

1. DeVon HA, Mirzaei S, Zègre-Hemsey J. Typical and atypical symptoms of acute coronary syndrome: Time to retire the terms? J Am Heart Assoc 2020;9:e015539.

doi: 10.1161/JAHA.119.015539.
2. Gulati M, Levy PD, Mukherjee D, Amsterdam E, Bhatt DL, Birtcher KK, et al. 2021 AHA/ACC/ASE/CHEST/SAEM/SCCT/ SCMR guideline for the evaluation and diagnosis of chest pain: A report of the American College of Cardiology/American Heart Association Joint Committee on clinical practice guidelines. Circulation 2021;144:e368-e454.
3. Hascoët S, Bongard V, Chabbert V, Marachet MA, Rousseau H, Charpentier S, et al. Early triage of emergency department patients with acute coronary syndrome: Contribution of 64-slice computed tomography angiography. Arch Cardiovasc Dis 2012;105:338-46.
4. Knuuti J, Wijns W, Saraste A, Capodanno D, Barbato E, Funck-Brentano C, et al. 2019 ESC guidelines for the diagnosis and management of chronic coronary syndromes. Eur Heart J 2020;41:407-77.
5. Krul MM, Bogaard K, Knol RJ, van Rossum AC, Knaapen P, Cornel JH, et al. Coronary artery disease in patients with atypical chest pain with and without diabetes mellitus assessed with coronary CT angiography. BMJ Open Diabetes Res Care 2014;2:e000004. doi: 10.1136/bmjdrc-2013-000004.
6. Han D, Lin A, Kuronuma K, Tzolos E, Kwan AC, Klein E, et al. Association of plaque location and vessel geometry determined by coronary computed tomographic angiography with future acute coronary syndrome-causing culprit lesions. JAMA Cardiol 2022;7:309-19.
7. Pugliese L, Spiritigliozzi L, Di Tosto F, Ricci F, Cavallo AU, Di Donna C, et al. Association of plaque calcification pattern and attenuation with instability features and coronary stenosis and calcification grade. Atherosclerosis 2020;311:150-7.
8. Motoyama S, Kondo T, Sarai M, Sugiura A, Harigaya H, Sato T, et al. Multislice computed tomographic characteristics of coronary lesions in acute coronary syndromes. J Am Coll Cardiol 2007;50:319-26.
9. Weigold WG, Abbara S, Achenbach S, Arbab-Zadeh A, Berman D, Carr JJ, et al. Standardized medical terminology for cardiac computed tomography: A report of the Society of Cardiovascular Computed Tomography. J Cardiovasc Comput Tomogr 2011;5:136-44.
10. van Rosendael AR, Cainzos-Achirica M, Al-Mallah MH. Calcified plaque morphology, density, and risk. Atherosclerosis 2020;311:100-2.
11. Maurovich-Horvat P, Hoffmann U, Vorpahl M, Nakano M, Virmani R, Alkadhi H. The napkin-ring sign: CT signature of high-risk coronary plaques? JACC Cardiovasc Imaging 2010;3:440-4.
12. Badimon L, Vilahur G. Thrombosis formation on atherosclerotic lesions and plaque rupture. J Intern Med 2014;276:618-32.
13. Camaré C, Pucelle M, Nègre-Salvayre A, Salvayre R. Angiogenesis in the atherosclerotic plaque. Redox Biol 2017;12:18-34.
14. Evrard S, Delanaye P, Kamel S, Cristol JP, Cavalier E. Vascular calcification: From pathophysiology to biomarkers. Clin Chim Acta 2015;438:401-14.
15. Divakaran S, Cheezum MK, Hulten EA, Bittencourt MS, Silverman MG, Nasir K, et al. Use of cardiac CT and calcium scoring for detecting coronary plaque: Implications on prognosis and patient management. Br J Radiol 2015;88:20140594. doi: 10.1259/bjr.20140594.
16. Mézquita AJV, Biavati F, Falk V, Alkadhi H, Hajhosseiny R, Maurovich-Horvat P, et al. Clinical quantitative coronary artery stenosis and coronary atherosclerosis imaging: A consensus statement from the quantitative cardiovascular imaging study group. Nat Rev Cardiol 2023;20:696-714.